An EPR, thermostability and pH-dependence study of wild-type and mutant forms of catechol 1,2 dioxygenase from Acinetobacter radioresistens S13

R. Caglio; E. Pessione; F. Valetti; C. Giunta; E.Ghibaudi. An EPR, thermostability and pH-dependence study of wild-type and mutant forms of catechol 1,2 dioxygenase from Acinetobacter radioresistens S13.
BIOMETALS. 26 pp: 75-84.
DOI: 10.1007/s10534-012-9595-x

BioMetals

An EPR, thermostability and pH-dependence study of wild-type and mutant forms of catechol 1,2 dioxygenase from Acinetobacter radioresistens S13

--Manuscript Draft--

Manuscript Number:	BIOM-D-12-01763
Full Title:	An EPR, thermostability and pH-dependence study of wild-type and mutant forms of catechol 1,2 dioxygenase from Acinetobacter radioresistens S13
Article Type:	Manuscript
Keywords:	EPR spectroscopy, structure-function relationships, intradiol dioxygenase, aromatic compound degradation, protein stability, iron-containing enzyme
Corresponding Author:	Elena Ghibaudi Torino, ITALY
Corresponding Author Secondary Information:	
Corresponding Author's Institution:	
Corresponding Author's Secondary Institution:	
First Author:	Raffaella Caglio, PhD
First Author Secondary Information:	
Order of Authors:	Raffaella Caglio, PhD
	Enrica Pessione, Professor
	Francesca Valetti, Assistant professor
	Carlo Giunta, Professor
	Elena Ghibaudi
Order of Authors Secondary Information:	
Abstract:	Intradiol dioxygenase are iron-containing enzymes involved in the bacterial degradation of natural and xenobiotic aromatic compounds. The wild-type and mutants forms of catechol 1,2 dioxygenase Iso B from Acinetobacter radioresistens LMG S13 have been investigated in order to get an insight on the structure-function relationships within this system. 4K CW-EPR spectroscopy highlighted different oxygen binding properties of some mutants with respect to the wild-type enzyme, suggesting that a fine tuning of the substrate-binding determinants in the active site pocket may indirectly result in variations of the iron reactivity. A thermostability investigation by optical spectroscopy, that reports on the state of the metal center, showed that the structural stability is more influenced by the type rather than by the position of the mutation. Finally, the influence of pH and temperature on the catalytic activity was monitored and discussed in terms of perturbations induced on the tertiary contacts network of the enzyme.

An EPR, thermostability and pH-dependence study of wild-type and mutant forms of catechol 1,2 dioxygenase from *Acinetobacter radioresistens S13*

Raffaella Caglio[1], Enrica Pessione[1], Francesca Valetti[1], Carlo Giunta[1], Elena Ghibaudi[2]*

[1]*Dipartimento di Scienze della Vita e Biologia dei Sistemi, Università di Torino, Via Accademia Albertina 13, 10123 Torino, Italy*

[2]*Dipartimento di Chimica, Università di Torino, via Giuria 7, 10125 Torino, Italy*

*corresponding author

Tel. ++39-011-6707951

Fax ++39-011-6707855

E-mail: elena.ghibaudi@unito.it

Abstract

Intradiol dioxygenase are iron-containing enzymes involved in the bacterial degradation of natural and xenobiotic aromatic compounds. The wild-type and mutants forms of catechol 1,2 dioxygenase Iso B from *Acinetobacter radioresistens* LMG S13 have been investigated in order to get an insight on the structure-function relationships within this system. 4K CW-EPR spectroscopy highlighted different oxygen binding properties of some mutants with respect to the wild-type enzyme, suggesting that a fine tuning of the substrate-binding determinants in the active site pocket may indirectly result in variations of the iron reactivity. A thermostability investigation by optical spectroscopy, that reports on the state of the metal center, showed that the structural stability is more influenced by the type rather than by the position of the mutation. Finally, the influence of pH and temperature on the catalytic activity was monitored and discussed in terms of perturbations induced on the tertiary contacts network of the enzyme.

Keywords: *EPR spectroscopy, structure-function relationships, intradiol dioxygenase, aromatic compound degradation, protein stability, iron-containing enzyme*

Abbreviations:

1,2-CTD: catechol 1,2 dioxygenase

Ar-1,2-CTD: catechol 1,2 dioxygenase Iso B from *A. radioresistens* S13

1,2-CCD: chlorocatechol 1,2 dioxygenase

4-CCD: chlorocatechol 1,2 dioxygenase from *R. opacus* 1CP

1.INTRODUCTION

Non-heme Fe dioxygenase, that are classified into extradiol and intradiol cleaving enzymes based on their catalytic mechanism, are of paramount importance for the bacterial degradation of natural and xenobiotic aromatic compounds (Furukawa 2000; Milligan 1998; Nishizuka 2006; Ogawa2003; Pieper 2000; Reinecke 1998].

Both classes catalyze the dearomatization of the substrate by inserting molecular oxygen in the aromatic ring and are characterized by the presence of Fe^{II} and Fe^{III} as the catalytic center, respectively.

The X-ray structures at 1.80 Á resolution of wild-type catechol 1,2 dioxygenase from *Acinetobacter radioresistens* LMG S13 and of its A72G mutant have been recently deposited in the Protein Data Bank (entries 2XSV and 2XSU) (Micalella 2011).

The catalytic center is a trigonal bipyramidal Fe^{III} ion coordinated by two histidine and two tyrosine residues and a water molecule in the equatorial plane as the fifth ligand. The axial tyrosine and the water ligand are displaced by catechol, allowing a direct coordination of the diol to the Fe^{III}, based on spectral (Horsman 2005; Citadini 2005) and crystallographic evidence (Citadini 2005; Earhart 2005; Ferraroni 2004; Ferraroni 2006; Matera 2010; Vetting 2000). According to the accounted models for the catalytic cycle, the oxygen binds directly to the iron centre (Bugg 2003) in an ordered sequential mechanism.

A basic issue concerning this class of enzymes is their substrate selectivity: although it is known to be influenced by electronic factors, a number of investigations prove that it is finely tuned by the active site residues (Caglio 2009; Ferraroni 2004; Ferraroni 2006; Matera 2010).

Some residue in the catalytic pocket have been shown crucial for catalysis (Ferraroni 2004; Vetting 2010): these are Asp52/Pro76, Ala53/Gly77, Phe78/Leu109 and Cys224/Ala254 (4-CCD from *R. opacus*/1,2-CTD *Acinetobacter* ADP1). Site-directed mutagenesis applied to positions 69 and 72 of the primary sequence of catechol 1,2 dioxygenase IsoB from *Acinetobacter radioresistens* LMG S13 (Caglio 2009; Caposio 2002) brought to the expression of the following mutants: Leu69Ala, Ala72Gly, Ala72Pro, Ala72Ser, Ala72Asn, Ala72Asp and the double mutant Leu69Gly Ala72Gly. It has been demonstrated (Caglio 2009) that mutants at pos.69 show a higher substrate specificity towards 4-chlorinated catechols and are active towards 4,5-dichlorocatechol and tert-butylcatechol, which are never or rarely recognized by 1,2 chlorocatechol dioxygenase (1,2-CCD) (Potrawfke 2001) or 1,2 catechol dioxygenase (1,2-CTD). Conversely mutations at pos.72 results in higher catalytic efficiency towards mono-chlorinated substrates.

In the present study, a CW-EPR investigation of the wild-type and mutants forms of Ar-1,2-CTD from *Acinetobacter radioresistens* LMG S13 has been carried out with a special focus on the oxygen binding mode of the different variants. The thermostability of these variants has also been monitored by UV-Vis spectroscopy, taking the iron centre as a marker. Finally the optimal Temperature and pH values for the catalytic activity have been checked in all variants and the results have been compared and discussed in the light of the structural data available on the enzyme.

2.EXPERIMENTALS

2.1 Chemicals

All reagents used in this study were analytical grade and were purchased from Sigma-Aldrich (Milan, Italy). Liquid helium was supplied by SIAD (Turin, Italy).

2.2 Protein expression and purification

Ar-1,2-CTD was expressed in *E. coli* BL21(DE3) as described elsewhere (Caglio 2009). The concentration of wt and recombinant protein was determined through the absorbance peaks at 280 and 430 nm, by using the extinction coefficients reported by Briganti et al. (2000) $\varepsilon_{280}^{1mg/ml}$=0.798 $\varepsilon_{430}^{1mg/ml}$=0.033 $\varepsilon_{440}^{1mg/ml}$=0.049. All UV-Vis measurements were performed on a diode-array spectrophotometer Agilent 8453 UV/visible equipped with a Peltier system for temperature control.

2.3 Electron Spin Resonance measurements

CW-EPR measurements were performed on a Bruker 300ESP instrument, equipped with a cylindrical cavity and a cryostat for measurements at liquid Helium (4K) temperature. The protein samples dissolved in 50mM HEPES buffer pH 8.0 were concentrated up to 1 mM on Amicon VIVASPIN ultrafilters and put into quartz tubes (Ø = 3 mm), that were subsequently frozen in liquid nitrogen and inserted into the cryostat for measurements. The instrumental settings were as follows: microwave power 2 mW; modulation amplitude 2 G; modulation freq. 100 KHz; T = 4 K; freq. 9.42 GHz. Saturation curves were determined with the same instrumental settings, except that microwave power was varied in the 80μW-10mW range.

2.4 Thermal unfolding studies

Thermal transitions were monitored in the 20-95°C range by using the absorption peak at 430 nm as a marker of the integrity of the iron catalytic centre. The wt and mutant samples in 50mM HEPES buffer pH 8.0 were concentrated up to 0.13 mM by ultrafiltration on Amicon VIVASPIN ultrafilters. Each sample was incubated for 3 minutes at the selected temperature and the absorbance at 430 nm was subsequently recorded. The same procedure was applied at each T.

2.5 Determination of the temperature of optimal activity

The catalytic activity of wt and variants of Ar-1,2-CTD was determined in the 10-60°C range after incubating each sample for 3 minutes at the chosen temperature.
The activity assay was performed spectrophotometrically by following the absorbance increase at 260 nm (ε =17600 $M^{-1}cm^{-1}$) due to the enzymatic conversion of catechol into *cis–cis* muconic acid.

1 ml solution contained: 0.1 μM (final concentration) Ar-1,2-CTD + catechol (concentration range = 1 μM-1 mM) in 50 mM HEPES buffer pH 8.0. The kinetic parameter (k_{cat}) was determined by fitting the experimental data to the Michaelis–Menten model by a non-linear least-squares fitting program. In order to ensure that the activity at increasing temperature was not affected by changes in K_M the substrates were always used in large excess (although comparison of K_M at 20 and 30°C on WT and mutants confirmed that no changes were observed on this parameter upon temperature increase).

2.6 Determination of the pH of optimal activity

The pH of optimal activity as well as the pH value corresponding to 50% residual activity of wt and variants of Ar-1,2-CTD were found by determining the k_{cat} values at 30°C over the 5.5-10.0 pH range, according to the above-described assay. The experimental conditions were the same as described above, apart from the buffer which was changed in order to cover the whole pH range. Twelve different buffers made by three compounds, MES (pH 5.5-7.5), HEPES (pH 7.5-8.5), CHES (pH 8.5-10.0) were prepared according to the result shown by an informatic tool (http://www.bioinformatics.org/JaMBW/5/4/index.html), setting the preparation temperature at 20°C and the working temperature at 30°C.
Buffer concentration was varied in order to keep a constant ionic strength of 0.033 M. At pH 7.5 and 8.5 both available buffer systems were used and the resulting data overlapped in order to confirm that there were no different effects of buffering compounds on the enzyme activity due to the chemical structure and not on the pH.

3. RESULTS

3.1 EPR measurements

The wild-type (wt) and mutant forms of Ar-1,2-CTD underwent EPR measurements at 4K, in order to find out whether mutations had a direct influence on the iron coordination sphere. In fact, EPR spectroscopy is extremely sensitive to the chemical and magnetic environment of paramagnetic ions and may report on distorsions and/or changes occurring within the iron coordination sphere.
The following samples were examined: wt, L69A, A72G, A72P, A72S, A72N, A72D and the double mutant L69G A72G. The EPR spectra are reported in Fig.1A and B: this is the first EPR report of a whole series of Ar-1,2-CTD mutants compared to the wt form.
All samples, with the only exception of A72D, were characterized by a signal at g~4.29 that is consistent with the presence of a Fe^{III} centre coordinated to Tyr and His in a ligand field rhombic (highly asymmetric) environment, in agreement with the data previously reported by Briganti *et al.* (1997). In the case of the wt enzyme, the sample was concentrated enough to exhibit the g~10

spectral minor component (data not shown) arising from the lowest energy Kramers doublet.
No iron signal was highlighted in the A72D mutant: this is indicative of a low level of iron incorporation that results in an Fe concentration lower than the sensitivity limit of EPR.
Unlike the spectra reported by Briganti *et al.* (1997)., the EPR traces denounce the massive presence of O_2 either dissolved or in close interaction with the iron center. O_2 dissolved in the buffer is responsible for the linebase distorsion and does not imply any specific interaction with the protein. Conversely, the two additional signals that appear as shoulders of the g~4.29 spectral line are typical of a magnetic interaction between paramagnetic centers (Cappillino 2012). As the only paramagnetic species found in the samples are O_2 and the Fe(III) ion, these signals are likely to arise from the interaction between these two species.
In order to establish the nature and the degree of lability of such interaction, the samples were thawed in a ice/water bath and degassed for several minutes under an Argon flux.
The spectral traces recorded on the degassed samples are reported in Fig.2A and B.
Dissolved oxygen was removed in all cases and, in most samples, the O_2 interacting with iron was removed as well, giving rise to EPR spectra similar to that reported by Briganti *et al.* (2000).
Although, a few exceptions were found. The shoulders of the g~4.29 EPR signal are still visible in both the L69A sample and the double mutant: this suggests a higher stability of their Fe-O_2 adduct as compared to the other samples. Their magnified EPR spectra are shown in Fig.3. Further attempts to degas the sample did not bring about any further change, thus showing that the interaction between O_2 and iron is relatively stable in these two cases.
Interestingly, samples that have lost the shoulders of the g~4.29 signal also underwent a colour change from bright red to pale red. Conversely, those that exhibited a stronger interaction with O_2 kept their bright colour unchanged. This provides an indirect evidence that O_2 enters the active site and is spatially very close to the iron.
The EPR spectra of the A72N mutant is also reported in Fig.3. The spectral pattern of this variant is completely distorted as compared to wt: this finding is consistent with a strong perturbation of the environment of the iron centre that results in an heterogeneous environment of the iron in this mutant.
In the attempt to further investigate the structural features of the iron environment and to determine the iron-ligand distances by pulsed EPR, the relaxation behaviour of all samples was investigated and the microwave saturation curves were determined at 4K (Fig.4). Different magnetic environments usually results in distinct relaxation behaviours: unfortunately, the iron centre of Ar-1,2-CTD turned out to be a very strong relaxing agent in all samples, thus making undistinguishable the relaxation times at 4K and preventing the pulsed-EPR approach.

3.2 Thermal denaturation studies

A difference in the stability of the iron coordination center of the different protein samples was detected as samples were thawed and frozen again: the intensity of the EPR signal arising from the iron centre was negatively affected, suggesting an iron loss. In order to quantify the thermal stability of the iron center, we determined the melting temperatures of wt Ar-1,2-CTD and its

mutant by using the absorption band at 430 nm as a marker of the state of the metal center, as this band reports specifically on the iron (Table 1).
Interestingly, we noticed meaningful stability differences between the wt and the mutants. Ar-1,2-CTD wt is the most stable form as it shows a melting temperature of about 48°C. All mutants were less stable; no direct correlation between the mutated position and the stability was found: for example, the L69A and the A72S forms display the same thermal stability, whereas A72G is slightly less stable. Interestingly, a similar marked decrease in thermal stability was observed in both the double mutant and the A72P variant: these two forms were the less stable of the whole family of mutants. No data were collected on A72N due to the extreme instability of the sample, that did not allow the application of the experimental protocol.

3.3 pH and temperature influence on the catalytic activity

In order to make a comparison between the catalytic performances of the wt and mutant forms of Ar-1,2-CTD, their optimal temperature, i.e. the temperature value corresponding to the highest enzyme activity (here referred to as optimal T values) were determined. These results are reported in Table 1, together with the corresponding k_{cat} values (determined in the presence of catechol).
As far as the optimal T values are concerned, no significant differences were noticed between the wt and the A72G or the A72P mutant. Conversely, mutation at position 69 seems to lower the T of optimal activity, as highlighted by the L69A and the double mutant form, although this latter is far less active. An opposite trend is followed by the A72S mutant, whose optimal T is several degree higher than the wt form. Interestingly, based on the k_{cat} values, this is also the most active mutant, although still half-active with respect to the wt. A possible stabilizing effect of hydrogen bonds to the serine residue inserted by the mutation could rationalise this finding.
In general, mutations at position 72 do not seem to be disrupting towards the catalytic activity of the enzyme, although in all cases their k_{cat} values are significantly lower as compared to wt. Mutations at position 69 affects the catalytic proficiency much more deeply, but it is also to be considered that mutation at that site enhances the recognition and catalysis towards 4-chlorocatechol by inverting the substrate preference (Caglio *et al.*, 2009).
Table 1 also reports the pH-dependence of k_{cat} for the wt and mutants forms of Ar-1,2-CTD enzyme, expressed either as pH of optimal activity or as pH corresponding to 50% residual activity (measured at 30°C).
The presence of mutations shifts or widens the pH range of optimal activity towards higher values (8.5-9.0).
As far as $pH_{50\%}$ is concerned, its value is shifted towards pH>7 in all cases, with the only exception of the A72P mutant, whose behaviour resembles that of wt. Once again, no correlation between the mutation site and the pH-dependence of the activity is found, whereas the type of mutation seems more crucial.

4. DISCUSSION

4.1 Oxygen binding properties

The EPR results show the presence of consistent oxygen amounts in the proteins samples. As oxygen was not detected in blank samples (containing the buffer, without the protein), it is clear that the increased oxygen concentration in the protein sample has to be related with the presence of the protein. Moreover, two clearly distinct behaviours were observed.

For most Ar-1,2-CTD variants, dioxygen could be removed by simple degassing: this went along with a marked colour change and the disappearance of the shoulders of the g~4.29 signal, clearly indicating that the interaction with dioxygen was extremely weak. A few samples still exhibited the shoulders of the g~4.29 signal even after repeated attempts to degas the sample under an Argon pressure; in addition these samples kept their color unchanged, providing an indirect evidence that the interaction between O_2 and iron is still in place and that it likely arises from the close proximity of the two paramagnetic species. This finding suggests an increased ability of the L69A and the double mutant to interact with oxygen and to form a moderately stable adduct.

These results may be interpreted in the light of the reaction mechanism of intradiol catechol dioxygenase and, in particular, of the detailed theoretical study by Nakatani et al**.** (2009). It is well known that the catalytic mechanism of intradiol catechol dioxygenase requires the activation of oxygen through an electron-transfer from the substrate, coordinated to the iron. Nakatani clearly shows that such charge-trasfer is possible only once the Fe(III)-O_2 bond is established, because it influences the energy level of the π_p* orbital of O_2. In other words, according to the "oxygen activation mechanism", once the catechol is in the active pocket, the dioxygen molecule directly attacks the iron center to form a η1-*end-on* type Fe(III)-O_2 adduct which is immediately converted into an iron(III)-η1-*end-on* superoxo species thanks to the charge-transfer from the catecholate moiety. The superoxo species quickly attacks the catechol moiety to give rise to the subsequent steps of the reaction mechanism (Bugg 2008). Interestingly the charge-transfer towards O_2 seems to occur without formation of iron(II) and may take place only when the Fe-O_2 distance becomes 2.4 Å or less. This is the key process of the dioxygen activation and is clearly influenced by the chemical environment of the iron within the catalytic pocket.

Thus, it seems clear that, once the substrate bound, the reaction of catechol dioxygenase implies a direct interaction of dioxygen with iron(III), in spite of the fact that – from a chemical point of view - this is usually unfavoured with respect to Fe(II), due to the ability of the latter to trigger the formation of an Fe(III)-superoxide stable complex.

All these findings suggest that the Fe(III)-oxygen interaction is possible and somehow assisted by the chemical environment.

Although in the absence of substrate, our experimental evidence of O_2 interaction with the iron center, in two Ar-1,2-CTD variants may be explained in the light of the structural perturbation induced by mutations. According to the Ar-1,2-CTD structure reported by Micalella *et al.* (2011), a weak water ligand is coordinated to the iron center and it is H-bonded to Arg216 in the wt form

of the enzyme. Mutations at positions 69 and 72 disrupt the H-bridge, further weakening the bond between water and the metal centre and promoting a perturbation of the tertiary contacts within the catalytic pocket that may results in the displacement of aminoacid residues. In addition, it is worth noting that the mutants that bind oxygen more strongly are those that, according to Micalella *et al.* (2011), are characterized by wider catalytic pockets. In fact, mutations at position 72 and 69 increases the pocket volume from 1.5 A^3 (wt) to 6.5 A^3 (A72G) and 10.6 A^3 (L69A), respectively. Such finding is supported by the unique ability of the L69A mutant to oxidise bulky substrates such as *tert*-butyl-catechol (Caglio 2009), which cannot be recognized by the wt or by the mutants at position 72. All in all, two factors may explain the increased ability of the L69A and the double mutant to interact with O_2, even in the absence of catechol: i) the higher accessibility of the metal site, due to the increased pocket volume, that may favour dioxygen diffusion towards the iron centre; ii) the perturbation of the tertiary contact networks, that may displace some residues belonging to the catalytic pocket and allow them to assist the formation of the adduct, resulting in an unexpected stabilization of the O_2-Fe adduct, even in the absence of catechol.

A72N is the only mutant whose EPR spectral pattern denounces a deep perturbation of the first coordination sphere of the metal, although pos.72 is not directly coordinated to the metal. The structural perturbation goes along with the peculiar catalytic behaviour of the A72N mutant (Caglio 2009), that is almost inactive with respect to other variants at the same sequence site. The replacement of Ala with Asn is likely to deeply affect the network of tertiary contacts surrounding position 72; the perturbation may propagate through the structure and reach the metal coordination site, thus explaining both the unusual spectral pattern and the loss of catalytic proficiency of this mutant.

4.2 Thermal stability

As far as the thermal stability issue is concerned, the experimental data show that it seems more influenced by the type than by the position of mutation. In fact, mutants L69A, A72S and A72G exhibit almost the same melting temperature in spite of the fact of bearing mutations at different sequence sites. Replacing Leu with Ala or Ala with Gly or Ser does not imply deep sterical perturbations, as the mutated residues occupy almost the same volume (or even a lower one) than the native ones. Polarity is not significantly affected, as well: the mutated residues are apolar or, in the case of Ser, slightly polar. This may provide a reason for their stability, which is only slightly lower as compared to wt.

Conversely, the A72P and the double mutant forms have more chances to bring about significant perturbations of the local environment of the mutation site. In fact, Pro is known to introduce abrupt torsions in the peptide backbone; on the other hand, a double mutation on two sites that are close in space is likely to disrupt the local network of tertiary contacts. This inevitably results in lower structural stability, as witnessed by the lower melting temperature found in these two systems.

The fact that a certain level of catalytic activity is maintained in both mutants and that their EPR spectra are quite similar to wt suggests that the perturbation affects only mildly the topology of the

first coordination sphere of the metal centre. Since the mutation sites are located in a region of the catalytic pocket that stabilizes the substrate by interacting with position 4 and 5 of the aromatic ring but are not very close to the residues that coordinate the iron atom the observed behaviour is consistent with a low impairment of the melting temperature which is estimated on the basis of the stability of the iron-protein interaction. The more pronounced effect highlighted on the double mutant can be affected by a significant decrease - in this mutant only - of the hydrophobicity of the pocket which can influence the iron retention, as discussed in Di Nardo *et al.* (2004)

4.3 Temperature and pH influence on the catalytic activity

A comparison between the melting temperatures and the T of optimal activity reported in Table 1 does not highlight cross-correlations between the two sets of values. The structural stability appears to be influenced by the kind of residue introduced by mutation, whereas both the T of optimal activity and the k_{cat} determined at that T seem more influenced by the localization of the mutation site. Position 72 is less crucial than pos. 69 in influencing the catalytic proficiency. This agrees with the experimental findings reported by Caglio *et al.* (2009), who found that the L69A mutant was less reactive towards catechol as compared to mutants on pos.72. This may also be related with the fact that Leu69 is strictly conserved in all intradiolic catechol dioxygenase. Interestingly, the peculiar behaviour of the A72S enzyme highlighted by Caglio *et al.* . (2009) is confirmed by our findings. In fact, this is the most active A72 mutant between those examined in this paper and it is also characterized by the highest T of optimal activity (37°C rather than the 30°C typical of the wt and the other A72 variants). Although a mechanistic explanation for this finding is not available, it seems possible that the presence of a Ser residue instead of an Ala may contribute to the stabilisation of the catalytic intermediates through the establishment of bonding interactions between the alcoholic function and the catechol or by a more general stabilisation of the active site through a rearranged hydrogen-bond network leading to stabilised intermediates that supports catalysis.

In general, most Ar-1,2-CTD samples are characterized by melting T significantly higher than their T of optimal activity. The only exception is represented by A72P enzyme, that exhibits a melting T surprisingly close to the T of optimal activity: apparently, in this specific case, the bulk of the protein may be destabilized to a good extent, without inducing the breakdown of the metal active site. This suggests that the metal center of Ar-1,2-CTD is one of the determinants of the protein stability. This is often the case in metalloproteins, where a catalytic core relatively resistant to thermal denaturation is surrounded by a more labile structural region (Boscolo 2009).

As for the effect of pH, experimental data once again do not highlight direct correlations between the position of mutations and the pH of optimal activity. This might be related with the fact that Ala72 or Leu69 do not undergo acid-base equilibria, i.e. they are insensitive to pH changes. The same is true for the residues found at these positions in the mutants, within the pH range scanned in our experiments.

If we look at the $pH_{50\%}$ values, the most original behaviour belongs once again to A72P, which is surprisingly similar to wt considering the highly perturbing effect of Pro on the backbone

structure. All mutations are characterized by $pH_{50\%}$ values 0.5-1.0 pH unit higher than wt. As the mutated residues are not involved in acid-base equilibria, this change has to be related with modifications of the tertiary interactions network which are likely to reflect on the protonation equilibria of the aminoacid closer to the iron site. A moderate and indirect effect, which is nonetheless very difficult to rationalize, can involve the action of pH on the substrate, since the Fe(III) catecholate complex is also expected to be modulated by the acid-base equilibria in the microenvironment surrounding the catalytic site.

5. CONCLUSIONS

The comparative EPR investigation of a series of Ar-1,2-CTD mutants has allowed us to highlight the effect of two mutations on oxygen binding properties of the enzyme. Our data prove that a perturbation of the environment of the catalytic pocket may result in an increased ability of the enzyme to interact with dioxygen.

A single mutant (A72N) denounces a structural perturbation that affects directly the first coordination sphere of the iron centre, whereas the A72D mutant turn out to be unable to bind iron and provides no EPR signal.

Finally, thermostability and pH studies shows that the structural stability of mutants appears to be influenced by the kind of residue introduced by mutation, whereas the catalytic parameters seem more influenced by the localization of the mutation site.

The experimental findings of this paper support those published by Caglio *et al.* (2009) and Micalella *et al.* (2011) and deepen our knowledge of the catechol dioxygenase structure-function relationships. They confirm the high degree of complexity of this enzyme, where small structural changes may result in impressive variations of the catalytic properties: this is witnessed by the specificity inversion found by Caglio *et al.* (2009) on the L69A mutant, which triggers the conversion of a catechol-dioxygenase into a chlorocatechol dioxygenase as for substrate selectivity.

Unraveling these aspects is of crucial importance for an enzyme that raises a high biotechnological interest due to its potential applications in the detection and removal of catechol derivatives from the environment.

References

Boscolo B., Leal S., Salgueiro C., Ghibaudi E.M., Gomes C.M. (2009) The prominent conformational plasticity of lactoperoxidase: a chemical and pH stability analysis. Biochim. Biophys. Acta 1794:1041–1048.

BrigantiF., Pessione E., Giunta C., Scozzafava A. (1997) Purification, biochemical properties and substrate specificity of a catechol-1,2-dioxygenase from a phenol degrading Acinetobacter radioresistens. FEBS Lett. 416: 61–64.

Briganti F., Pessione E., Giunta C., Mazzoli R., Scozzafava A.. (2000) Purification and Catalytic Properties of Two Catechol 1,2-Dioxygenase Isozymes from Benzoate-Grown Cells of Acinetobacter radioresistens. J. Protein Chem. 19: 709–716.

Bugg T.D.H. (2003) Dioxygenase enzymes: catalytic mechanisms and chemical models. Tetrahedron 59: 7075–7101.

Bugg T.D.H, Ramaswamy S. (2008) Non-heme iron-dependent dioxygenases: unravelling catalytic mechanisms for complex enzymatic oxidations. Curr. Opin.Chem.Biol., 12:134–140

Caglio R., Valetti F., Caposio P., Gribaudo G., Pessione E., Giunta C. (2009) Fine-Tuning of Catalytic Properties of Catechol 1,2-Dioxygenase by Active Site Tailoring. Chem. Bio. Chem. 10:1015–1024.

Caposio P., Pessione E., Giuffrida G., Conti A., Landolfo S., Giunta C., Gribaudo G. (2002) Cloning and characterization of two catechol 1,2-dioxygenase genes from Acinetobacter radioresistens S13. Res. Microbiol. 153: 69–74.

Cappillino P.J., Miecznikowski J.R., Tyler L.A., Tarves P.C., McNally J.S., Bala W.L., Kasibhatla S.T. Krzyaniak M.D., McCracken J., Wang F. Armstrong W.H., J.P. Caradonna (2012) Studies of iron(II) and iron(III) complexes with *fac*-N_2O, cis-N_2O_2 and N_2O_3 donor ligands: models for the 2-His 1-carboxylate motif of non-heme iron monooxygenases. Dalton Trans. 41: 5662–5677.

Citadini A.P.S., Pinto A.P.A, Araújo A.P.U., Nascimento O.R., Costa-Filho A.J. (2005) EPR studies of chlorocatechol 1,2-dioxygenase: evidences of iron reduction during catalysis and of the Binding of Amphipatic Molecules. Biophys. J. 88: 3502–3508.

Di Nardo G., Pessione E., Cavaletto M., Anfossi L., Vanni A., Briganti F., Giunta C. (2004) Effects of surface hydrophobicity on the catalytic iron ion retention in the active site of two catechol 1,2-dioxygenase isoenzymes. Biometals. 17: 699-706.

Earhart C.A., Vetting M.W., Gosu R., Michaud-Soret I., Que L., Ohlendorf D.H., (2005) Structure of catechol 1,2-dioxygenase from Pseudomonas arvilla. Biochem. Biophys. Res. Commun. 338: 198–205.

Ferraroni M., Solyanikova I.P., Kolomytseva M.P., Scozzafava A., Golovleva L., Briganti F. (2004) Crystal structure of 4-chlorocatechol 1,2-dioxygenase from the chlorophenol-utilizing Gram-positive Rhodococcus opacus 1CP. J. Biol. Chem. 79: 27646–27655.

Ferraroni M., Kolomytseva M.P., Solyanikova I.P., Scozzafava A., Golovleva L.A., Briganti F. (2006) Crystal Structure of 3-Chlorocatechol 1,2-dioxygenase key Enzyme of a New Modified Ortho-pathway from the Gram-positive Rhodococcus opacus 1CP Grown on 2-chlorophenol J. Mol. Biol. 360: 788–799.

Furukawa K. (2000) Biochemical and genetic bases of microbial degradation of polychlorinated biphenyls (PCBs). J. Gen. Appl. Microbiol. 46: 283–296.

HorsmanG.P., Jirasek A., Vaillancourt F.H., Barbosa C.J. , Jarzecki A.A., Xu C., Mekmouche Y., Spiro T.G., Lipscomb J.D., Blades M.W., Turner R.F., Eltis L.D. (2005) Spectroscopic studies of the anaerobic enzyme-substrate complex of catechol 1,2-dioxygenase. J. Am. Chem. Soc. 48:16882–16891.

Matera I., Ferraroni M., Kolomytseva M., Golovleva L., Scozzafava A., Briganti F. (2010) Catechol 1,2-dioxygenase from the Gram-positive Rhodococcus opacus 1CP: quantitative structure/activity relationship and the crystal structures of native enzyme and catechols adducts. J. Struct. Biol. 170:548–564.

Micalella C., Martignon S., Bruno S., Pioselli B., Caglio R., Valetti F., Pessione E., Giunta C., Rizzi M. (2011) X-ray crystallography, mass spectrometry and single crystal microspectrophotometry: A multidisciplinary characterization of catechol 1,2 dioxygenase. Biochim. Biophys. Acta 1814: 817–823.

Milligan P.W., Haggblom M.M. (1998) Biodegradation of resorcinol and catechol by denitrifying enrichment cultures. Environ. Toxicol. Chem. 17:1456–1461.

Nakatani N., Nakao Y., Sato H., Sakaki S. (2009) Theoretical Study of Dioxygen Binding Process in Iron(III) Catechol Dioxygenase: “Oxygen Activation” vs “Substrate Activation”. J. Phys. Chem. B, 113: 4826–4836)

Nishizuka Y., Ichiyama A., Nakamura S., Hayaishi O. (1962) A new metabolic pathway of catechol, J. Biol. Chem. 237: C268–C270.

Ogawa N., Miyashita K., Chakrabarty A.M. (2003) Microbial genes and enzymes in the degradation of chlorinated compounds. Chem. Rec. 3:158–171.

Pieper D.H., Reineke W. (2000) Engineering bacteria for bioremediation. Curr. Opin. Biotechnol. 11: 262–270.

Potrawfke T., Armengaud J., Wittich R.M. (2001) Chlorocatechols substituted at positions 4 and 5 are substrates of the broad-spectrum chlorocatechol 1,2-dioxygenase of Pseudomonas chlororaphis RW71. J. Bacteriol. 183: 997–1011.

Reineke W. (1998) Development of hybrid strains for the mineralization of chloroaromatics by patchwork assembly. Annu. Rev. Microbiol. 52: 287–331.

Vetting M.W., Ohlendorf D.H. (2000) The 1.8 Å crystal structure of catechol 1,2-dioxygenase reveals a novel hydrophobic helical zipper as a subunit linker. Struct. Fold. Des. 8: 429–440.

Table1: Thermal stability values, pH and T dependence of the wild-type and mutant forms of Ar-1,2-CTD

Column: 1) Melting T of Ar-1,2-CTD wt and variants determined by monitoring the optical absorption at 430 nm; 2) T of optimal activity and corresponding k_{cat} value; 3) pH of optimal activity at 30°C; 4) pH values corresponding to 50% residual activity at 30°C.

	1	**2**	**3**	**4**
Protein variant	**Melting Temperature (°C)**	**T of optimal activity (°C) and k_{cat} (s^{-1})**	**pH of optimal activity (catechol)**	**$pH_{50\%}$ (catechol)**
WT	48.2 ± 0.2	30°C 30.03 ± 1.77	8.0-8.5	6.89 ± 0.05*
L69A	45.4 ± 0.8	27°C 4.81 ± 0.10	8.0-9.0	7.07 ± 0.07*
A72G	43.6 ± 0.2	30°C 13.56 ± 2.61	9.0	7.44 ± 0.05*
A72P	36.8 ± 0.5	30°C 14.27 ± 0.16	8.5-9.0	6.57 ± 0.02
A72S	45.6 ± 0.2	37°C 15.48 ± 0.51	8.0-9.0	7.53 ± 0.06*
L69G A72G	37.9 ± 0.7	23°C-27°C 2.04 ± 0.27	8.0	7.49 ± 0.25*

* data adapted from Caglio et al. (2009)

Figure captions

Figure 1A and B – 4K EPR spectra of Ar-1,2-CTD wt and variants in 50mM HEPES solution pH 8.0 before degassing. The signal at g=4.29 raises from the iron coordination centre. The spectra show signals assignable to oxygen either dissolved in the buffer or in magnetic interaction with the iron. Experimental settings: microwave power 2 mW; modulation amplitude 2 G; freq. 9.42 GHz.

Figure 2A and B – 4K EPR spectra of Ar-1,2-CTD wt and variants in 50mM HEPES solution pH 8.0 after degassing with Argon. The signal at g=4.29 raises from the iron coordination centre. The oxygen dissolved in the buffer has disappeared and only L69A and the double mutant forms still show the presence of oxygen interacting with the iron. Experimental settings: microwave power 2 mW; modulation amplitude 2 G; freq. 9.42 GHz.

Figure 3 – 4K EPR spectra of three variants of Ar-1,2-CTD in 50mM HEPES solution pH 8.0 after degassing with Argon. The spectra of the L69A and the L69G A72G forms highlight the presence of oxygen in magnetic interaction with the iron; the spectral pattern associated with the A72N form indicates a strong perturbation of the iron coordination sphere.

Figure 4 – Saturation plot of Ar-1,2-CTD wt and variants in 50mM HEPES solution pH 8.0 after degassing with Argon, based on the intensity of the g=4.29 EPR signal recorded at 4K.

Figure 1

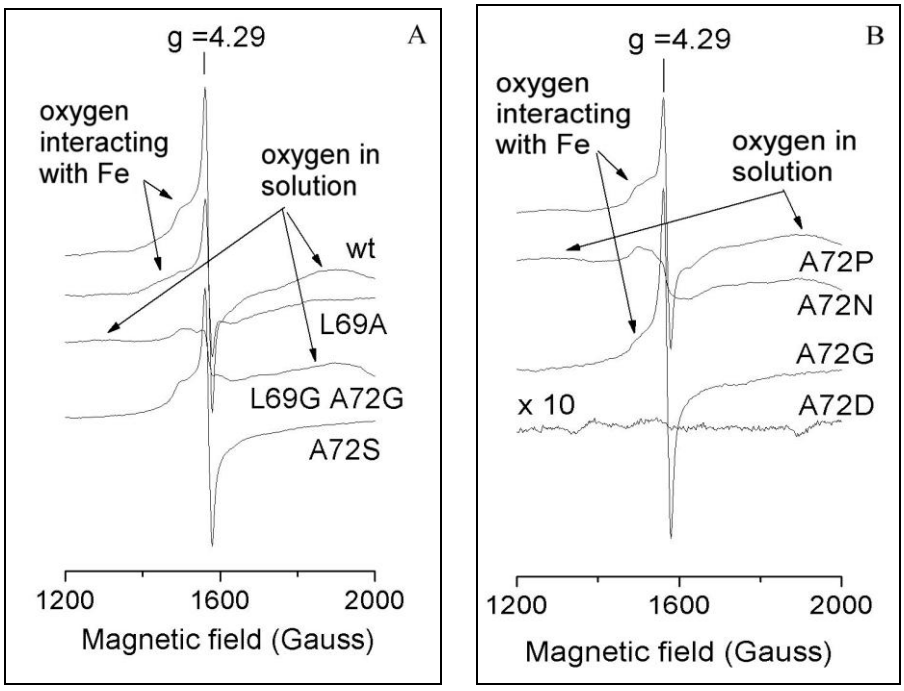
g =4.29
A
oxygen interacting with Fe
oxygen in solution
wt
L69A
L69G A72G
A72S
1200
1600
2000
Magnetic field (Gauss)
g =4.29
B
oxygen interacting with Fe
oxygen in solution
A72P
A72N
A72G
x 10
A72D
1200
1600
2000
Magnetic field (Gauss)

Figure 2

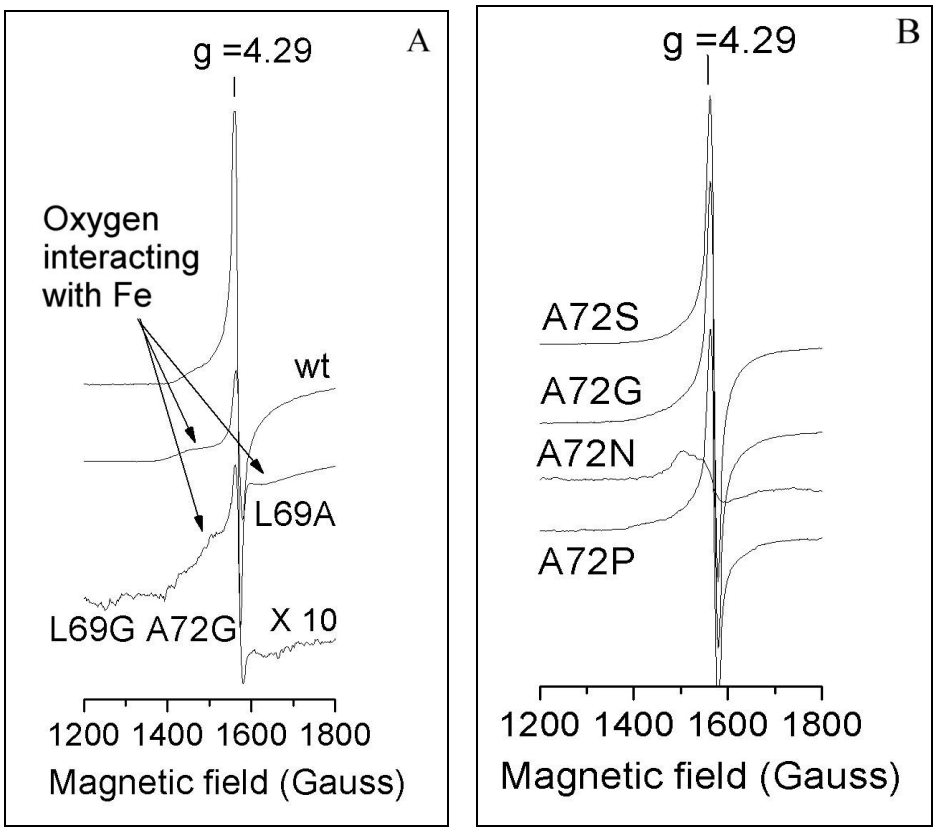
A
g =4.29
Oxygen
interacting
with Fe
wt
L69A
L69G A72G
X 10
1200 1400 1600 1800
Magnetic field (Gauss)
B
g =4.29
A72S
A72G
A72N
A72P
1200 1400 1600 1800
Magnetic field (Gauss)

Figure 3

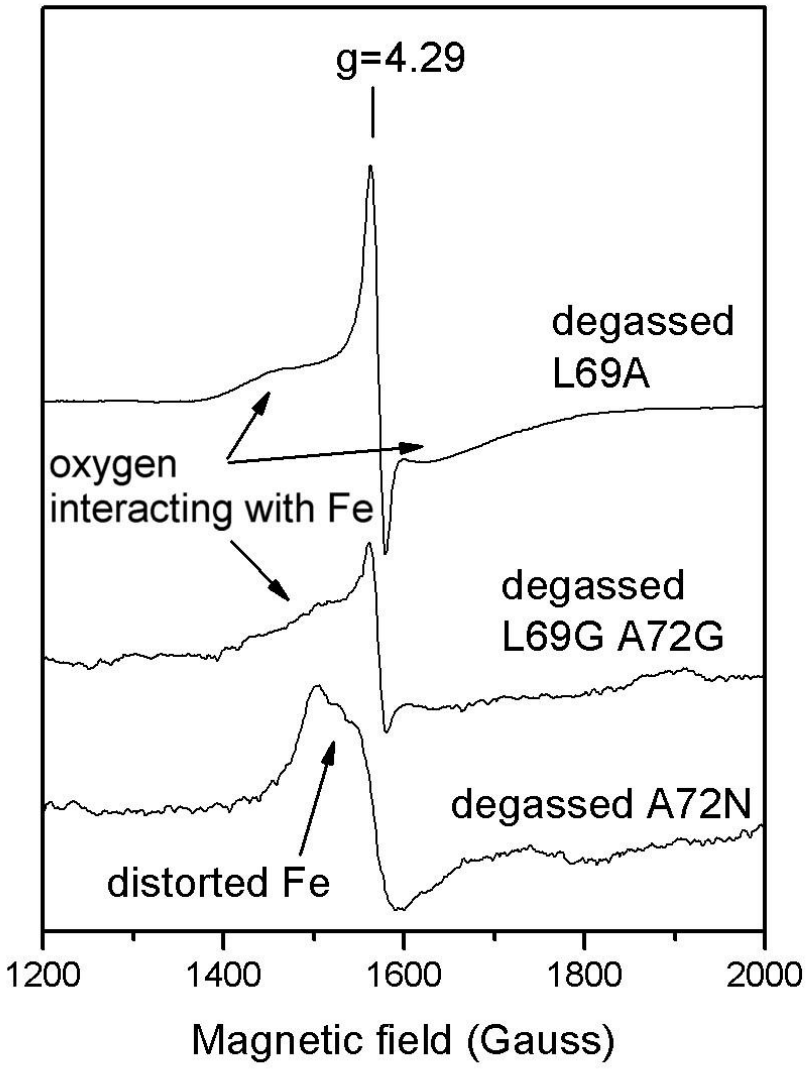
g=4.29
degassed
L69A
oxygen
interacting with Fe
degassed
L69G A72G
degassed A72N
distorted Fe
1200
1400
1600
1800
2000
Magnetic field (Gauss)

Figure 4

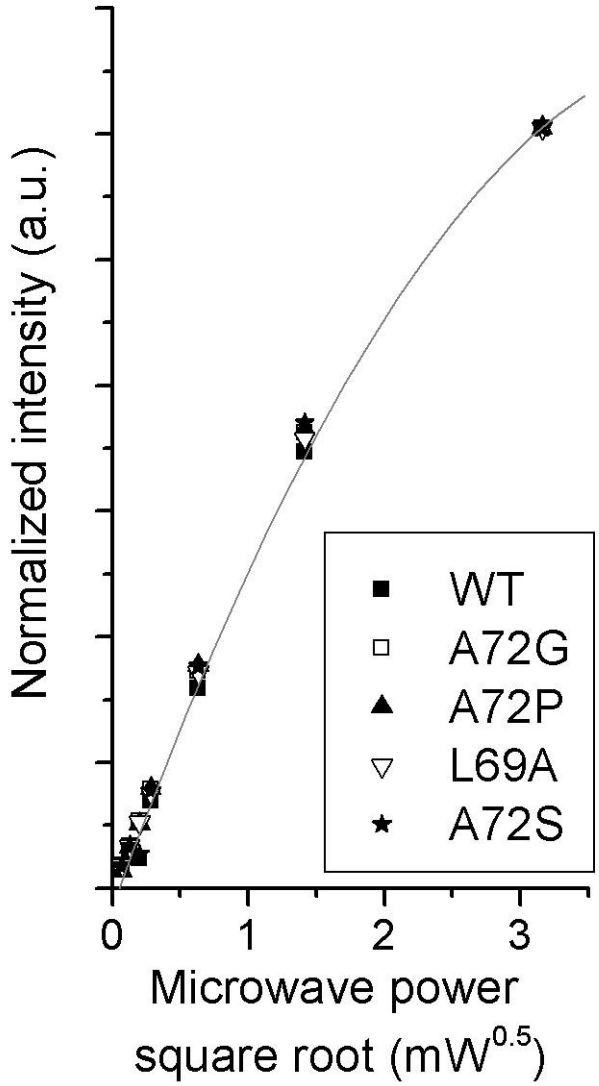
Normalized intensity (a.u.)
WT
A72G
A72P
L69A
A72S
0
1
2
3
Microwave power
square root (mW^0.5)

Figure 1A
Click here to download high resolution image

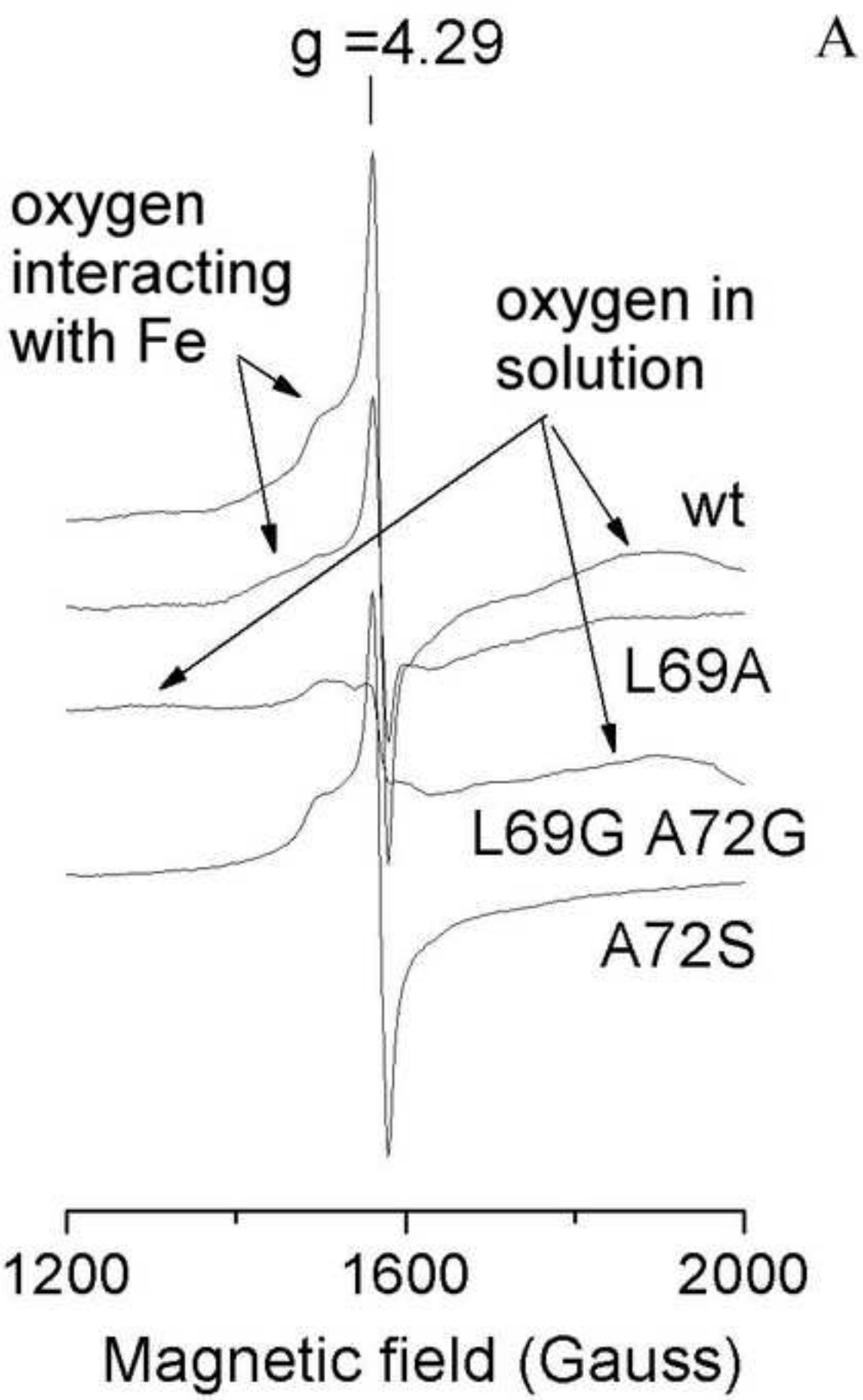

Figure 1B
Click here to download high resolution image

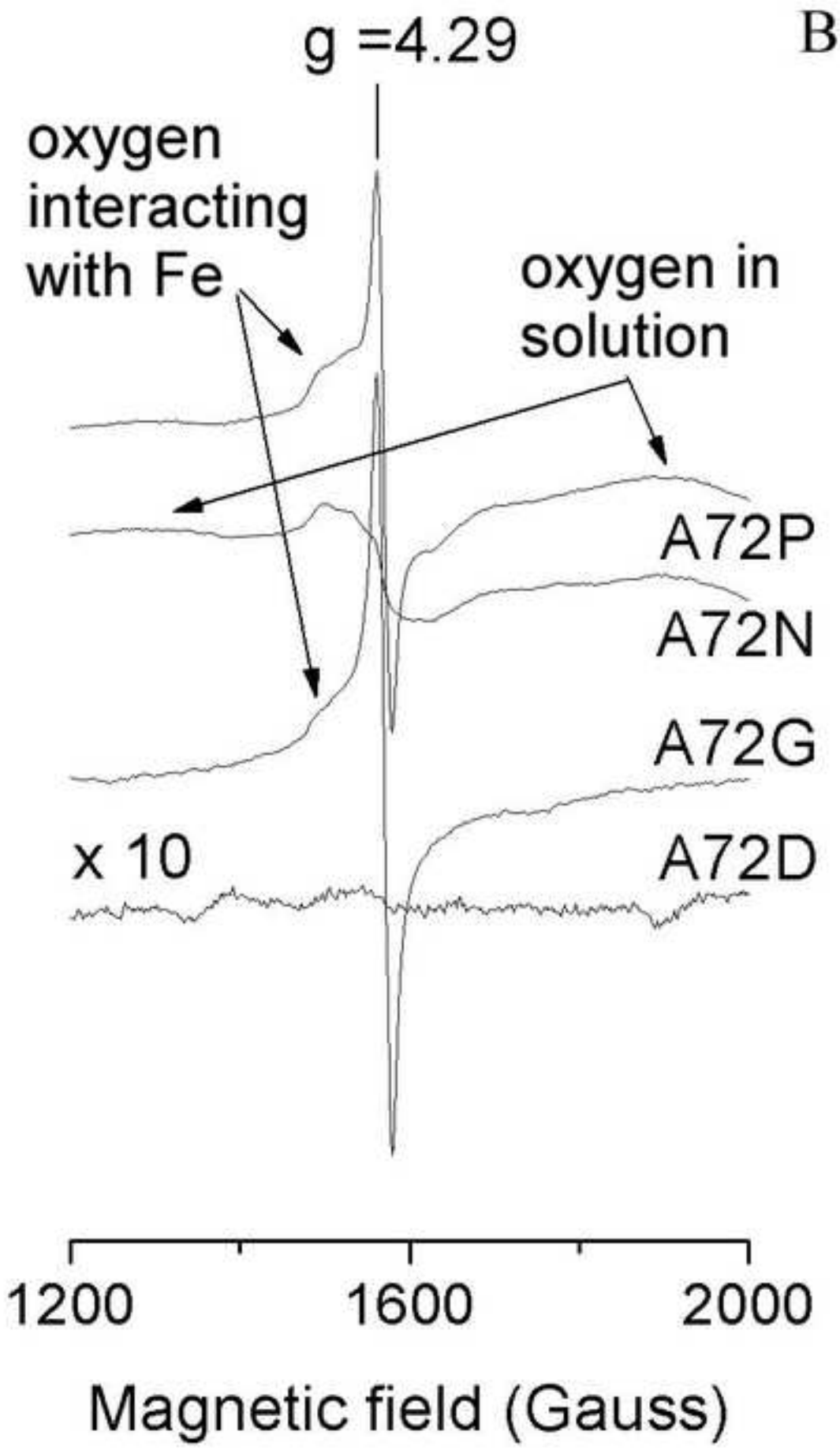

Figure 2A
Click here to download high resolution image

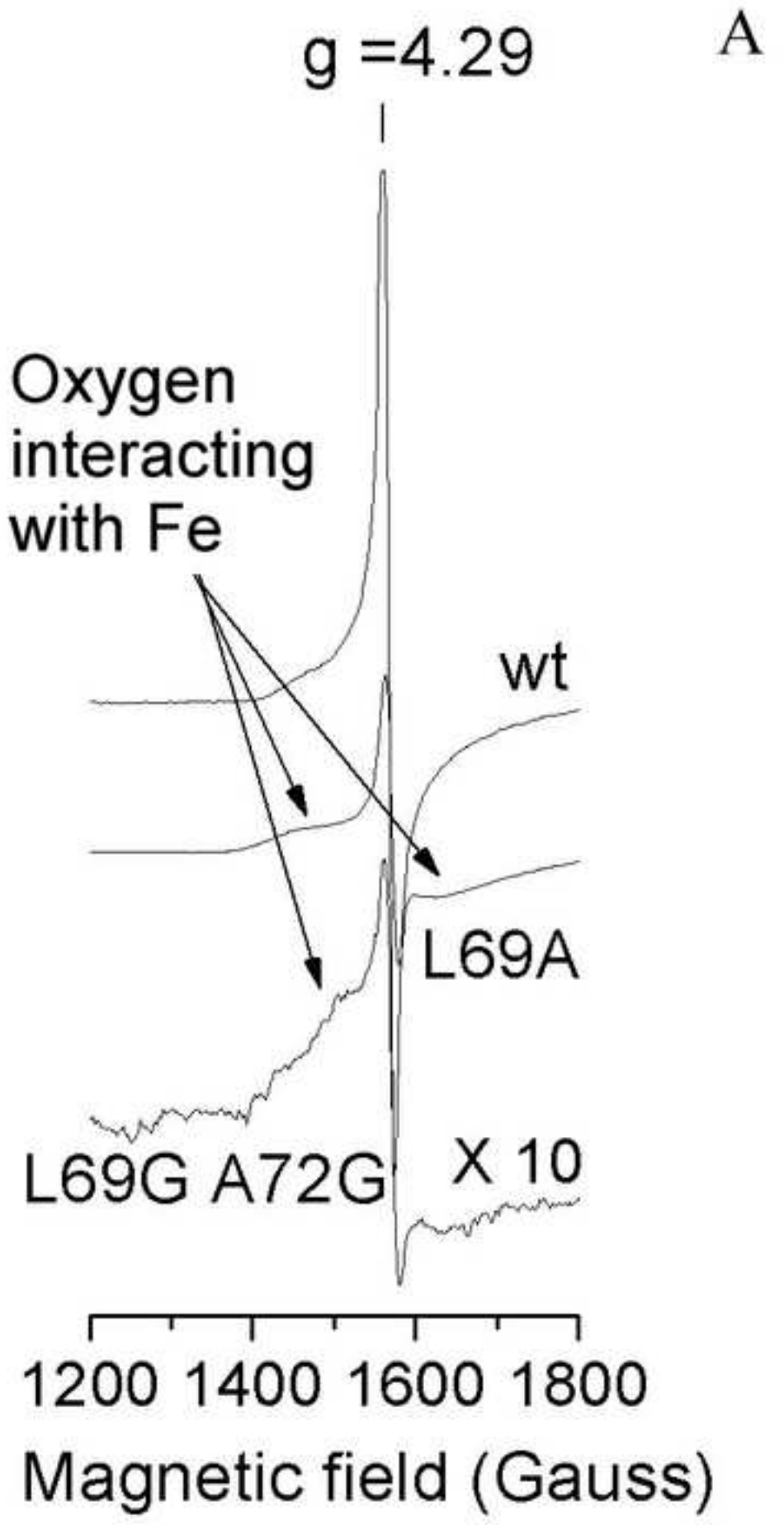

Figure 2B
Click here to download high resolution image

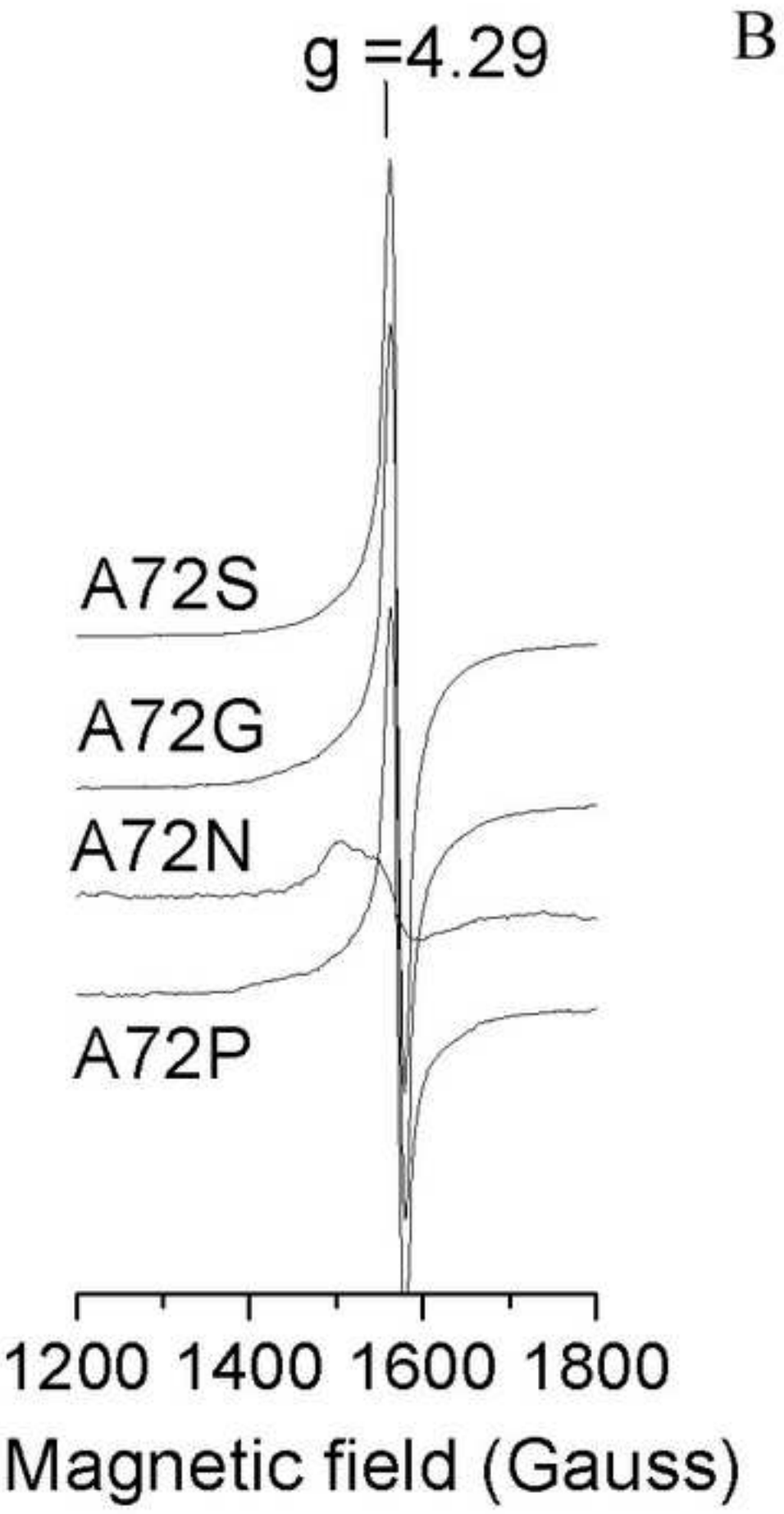

Figure 3
Click here to download high resolution image

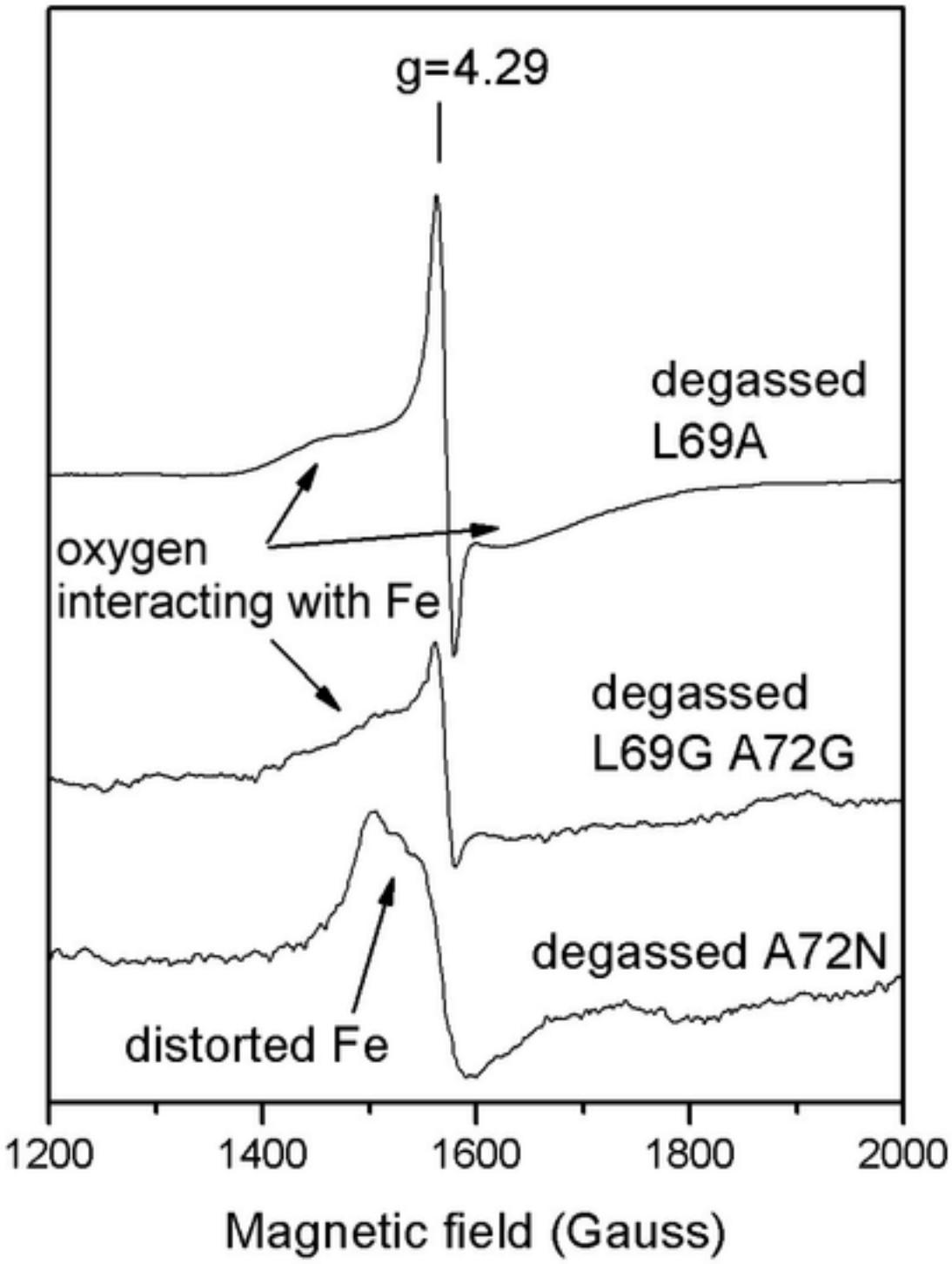

Figure 4
Click here to download high resolution image

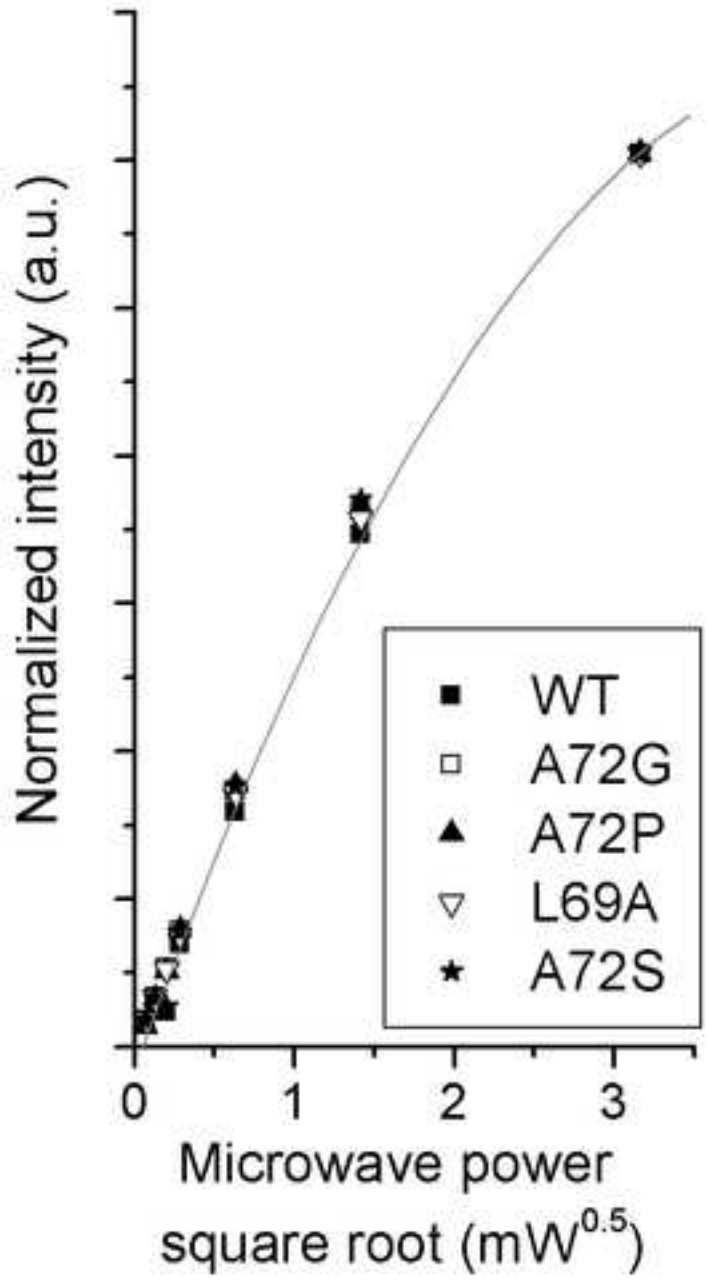

table 1
Click here to download table: Table1.doc

Table1: Thermal stability values, pH and T dependence of the wild-type and mutant forms of Ar-1,2-CTD

Column: 1) Melting T of Ar-1,2-CTD wt and variants determined by monitoring the optical absorption at 430 nm; 2) T of optimal activity and corresponding k_{cat} value; 3) pH of optimal activity at 30°C; 4) pH values corresponding to 50% residual activity at 30°C.

	1	**2**	**3**	**4**
Protein variant	**Melting Temperature (°C)**	**T of optimal activity (°C) and k_{cat} (s^{-1})**	**pH of optimal activity (catechol)**	**$pH_{50\%}$ (catechol)**
WT	48.2 ± 0.2	30°C 30.03 ± 1.77	8.0-8.5	6.89 ± 0.05*
L69A	45.4 ± 0.8	27°C 4.81 ± 0.10	8.0-9.0	7.07 ± 0.07*
A72G	43.6 ± 0.2	30°C 13.56 ± 2.61	9.0	7.44 ± 0.05*
A72P	36.8 ± 0.5	30°C 14.27 ± 0.16	8.5-9.0	6.57 ± 0.02
A72S	45.6 ± 0.2	37°C 15.48 ± 0.51	8.0-9.0	7.53 ± 0.06*
L69G A72G	37.9 ± 0.7	23°C-27°C 2.04 ± 0.27	8.0	7.49 ± 0.25*

* data adapted from Caglio et al. (2009)